HHS Public Access

Author manuscript

Dev Biol. Author manuscript; available in PMC 2022 September 01.

Published in final edited form as:

Dev Biol. 2021 September ; 477: 251–261. doi:10.1016/j.ydbio.2021.06.003.

Essential function and targets of BMP signaling during midbrain neural crest delamination

Michael L. Piacentino[1], **Erica J. Hutchins**[1], **Marianne E. Bronner**[1,*]

[1]Division of Biology and Biological Engineering, California Institute of Technology, Pasadena, California, USA

Abstract

BMP signaling plays iterative roles during vertebrate neural crest development from induction through craniofacial morphogenesis. However, far less is known about the role of BMP activity in cranial neural crest epithelial-to-mesenchymal transition and delamination. By measuring canonical BMP signaling activity as a function of time from specification through early migration of avian midbrain neural crest cells, we found elevated BMP signaling during delamination stages. Moreover, inhibition of canonical BMP activity via a dominant negative mutant Type I BMP receptor showed that BMP signaling is required for neural crest migration from the midbrain, independent from an effect on EMT and delamination. Transcriptome profiling on control compared to BMP-inhibited cranial neural crest cells identified novel BMP targets during neural crest delamination and early migration including targets of the Notch pathway that are upregulated following BMP inhibition. These results suggest potential crosstalk between the BMP and Notch pathways in early migrating cranial neural crest and provide novel insight into mechanisms regulated by BMP signaling during early craniofacial development.

Graphical Abstract

*corresponding author: mbronner@caltech.edu.

Author Contributions

Conceptualization: M.L.P., E.J.H., and M.E.B.
Experiment design: M.L.P. and E.J.H.
Experimentation: M.L.P. and E.J.H.
Data analysis: M.L.P.
Data interpretation: M.L.P., E.J.H., and M.E.B.
Manuscript preparation: M.L.P.
Manuscript editing: M.E.B. and E.J.H.

Competing Interests

The authors declare no competing interests.

Data and Code Availability

All source data and associated code used for analysis are publicly available on GitHub at https://github.com/mpiacentino/Transcriptome-profiling-reveals-BMP-target-genes-during-midbrain-neural-crest-delamination. Raw RNA-seq results are available in the following NCBI BioProjects: Control replicates BioProject #PRJNA673315 (performed in collaboration with (Hutchins et al., 2021)), and dnBMPR1A-FLAG replicates BioProject #PRJNA717985.

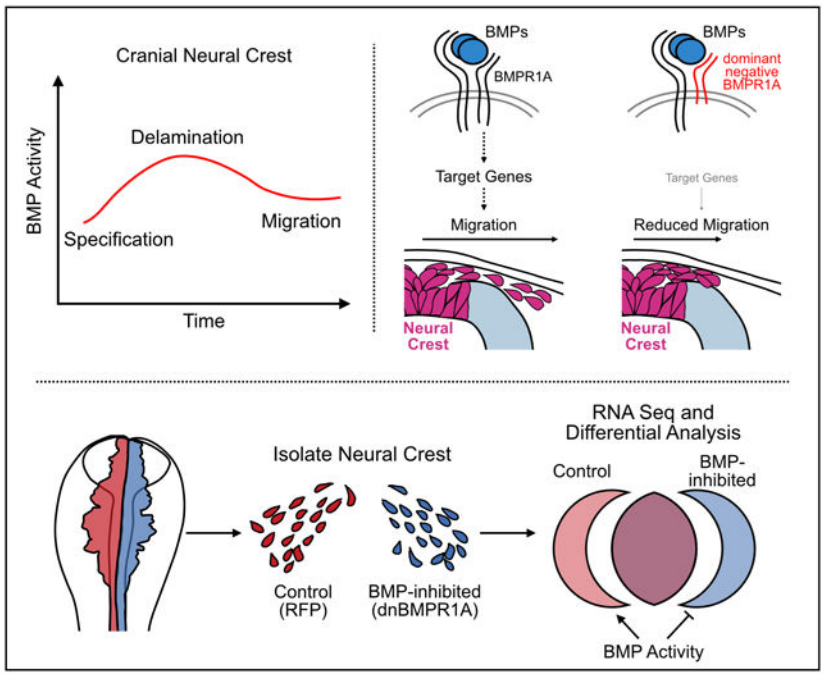

Keywords

Neural crest; Epithelial-to-mesenchymal transition; BMP signaling; RNA Seq; Delamination; Migration

Introduction

The neural crest is a multipotent stem cell population that undergoes an epithelial-to-mesenchymal transition (EMT) to migrate away from the forming central nervous system and differentiate into many essential cell types throughout the developing vertebrate body. While all neural crest cells share largely similar induction and specification events, their position along the anterior-posterior axis confers unique differentiation potentials depending upon their axial level of origin (Gandhi and Bronner, 2018; Hutchins et al., 2018; Martik and Bronner, 2017; Piacentino et al., 2020b); these subpopulations also display different mechanisms of EMT (Kalcheim, 2015; Theveneau and Mayor, 2012). Cranial neural crest cells originating from the forebrain, midbrain, and hindbrain are essential for craniofacial development and contribute to the bone and cartilage of the face and skull (Couly et al., 1993; le Douarin et al., 2004; Noden, 1983; Simoes-Costa and Bronner, 2016). Accordingly, dysregulation of cranial neural crest development frequently results in atypical craniofacial development (Siismets and Hatch, 2020; Vega-Lopez et al., 2018). Thus, studies of cranial neural crest development will contribute to better understanding and potential prevention of neurocristopathies.

BMP signaling has been implicated reiteratively in phases of cranial neural crest development including induction (Araya et al., 2009; Marchant et al., 1998; Pegge et al., 2019; Piacentino and Bronner, 2018; Schumacher et al., 2011; Tríbulo et al., 2003; Wu et al.,

2011; Yang et al., 2011), migration (Cheah et al., 2013; Goldstein et al., 2005; McLennan et al., 2017; Park and Gumbiner, 2010; Sela-Donenfeld and Kalcheim, 2000, 1999), survival (Graham et al., 1994; Hsu et al., 2016), differentiation, and craniofacial morphogenesis (Das and Crump, 2012; Dudas et al., 2004; Kanzler et al., 2000; Komatsu et al., 2013a, 2013b). In avian embryos, BMP signaling regulates delamination of the trunk neural crest (Cheah et al., 2013; Park and Gumbiner, 2010; Sela-Donenfeld and Kalcheim, 2000, 1999), and of the caudal cranial neural crest originating from the hindbrain (McLennan et al., 2017).

Our previous work has shown that Wnt signaling induces numerous transcriptional changes necessary for EMT in avian midbrain neural crest cells, including upregulation of *BMP4* and its canonical target *MSX1* (Hutchins et al., 2021). This raised a question regarding the potential role of BMP signaling during neural crest EMT from the midbrain, an area that was not well understood. In examining the time course of BMP activity at the midbrain level, our results show that activity peaks during neural crest delamination. Consistent with this, we find that BMP signaling is required for appropriate cranial neural crest migration. Transcriptome profiling analysis further identifies both positive and negative targets of BMP signaling during midbrain neural crest delamination. Together, these results demonstrate an important role for BMP signaling during neural crest emigration at the midbrain and provide insight into the cellular mechanisms regulated by BMP during early craniofacial development.

Results

Canonical BMP signaling peaks during cranial neural crest cell delamination

In order to measure the relative activity of the BMP signaling pathway in neural crest cells of the avian midbrain over time, we turned to a transcriptional reporter strategy in which conserved BMP-responsive cis-regulatory elements (BRE) from the *ID1* gene (le Dréau et al., 2012) were used to drive expression of nuclear-localized, destabilized EGFP (BRE::H2B-d2EGFP, Figure 1A. We electroporated chicken embryos with BRE::H2B-d2EGFP and quantitated BRE activity as a function of fluorescence intensity in individual midbrain neural crest cells during: 1. neural crest specification (6ss); 2. EMT and delamination (7–8ss); and 3. early migration (9–11ss) stages (Figure 1B).

The results show a progressive increase in BMP signaling activity within the midbrain neural crest cells as they transition from specification (6ss; Figure 1C1,D) through EMT and early migration (8ss; Figure 1C2,D). As neural crest cells continued their migration away from the neural tube, BMP signaling decreased (10ss; Figure 1C3,D). Within a given stage we observed similar BMP activity in both premigratory and migratory neural crest cells (Figure 1D), suggesting that the neural crest cell population responds to stage-specific BMP thresholds. Together, these results indicate that BMP signaling is relatively low at stages correlating with completion of neural crest specification, but then is redeployed during midbrain neural crest EMT. This suggests a potentially critical activity of BMP signaling during neural crest EMT at the midbrain level.

BMP signaling is required for early midbrain neural crest migration

We next sought to inhibit BMP signaling during midbrain neural crest EMT. Several BMP ligands, including BMP2, BMP4, BMP5, and BMP7 are all expressed in the forming chick head (Andrée et al., 1998; Bothe et al., 2011; Streit and Stern, 1999; Williams et al., 2019) and thus could be contributing to activation of BMP signaling targets during neural crest delamination. Since these ligands converge on the same Type I receptor, BMPR1A (Miyazono et al., 2010), we designed a strategy to inhibit BMP signaling at the level of this receptor to achieve a global BMP inhibition effect. To this end, we produced a dominant-negative BMPR1A construct lacking the cytoplasmic kinase domains and tagged with a FLAG epitope (dnBMPR1A-FLAG, Figure 2A) that also contained a downstream self-cleaving 2a peptide followed by cytoplasmic RFP for lineage tracing. This truncated receptor binds to extracellular BMP ligands but lacks the cytoplasmic kinase domains, preventing the activation of downstream intracellular responses (Maéno et al., 1994; Suzuki et al., 1994). Electroporation of this construct produced membrane-localized FLAG immunostaining, consistent with expected BMPR1A localization, and cytoplasmic RFP expression, indicating successful protein expression from this construct (Supplemental Figure S1A). Finally, BMP signal transduction indicated by phosphorylation of SMAD1/5/8 (pSMAD1/5/8) was reduced in the neural crest domain following dnBMPR1A-FLAG electroporation (Supplemental Figure S1B), confirming that this construct inhibits canonical BMP signaling.

We next tested the effect of BMP signaling inhibition on midbrain neural crest EMT. For these experiments, we performed bilateral electroporation of the control RFP construct on the left and the dnBMPR1A-FLAG construct (Figure 2A) on the right side of gastrulating chicken embryos, together with the *FOXD3* NC1.1m3 enhancer construct (Simões-Costa et al., 2012) which drives EGFP expression in specified cranial neural crest cells (NC1.1m3::EGFP). We incubated these embryos to early migration stages (8ss) at which point we immunolabeled for SNAI2 expression as a marker for delaminating and early migratory neural crest cells (Figure 2B). Interestingly, we found that loss of BMP signaling at EMT stages resulted in reduced neural crest migration area compared to the contralateral control sides (Figure 2C). These results suggest that BMP signaling is required for midbrain neural crest migration.

We then asked if the role of BMP signaling in neural crest migration is cell autonomous, or if it reflects a loss of BMP signaling in the surrounding embryonic tissue. To determine the autonomy of this effect, we performed dorsal neural tube explant experiments from embryos electroporated with 2a-RFP or with dnBMPR1A-FLAG and cultured these explants for 24 hours to allow neural crest cells to migrate away from the explanted tissue (Figure 2D). We measured the change in explant area between 2 and 24 hours post explant and found that neural crest cells expressing dnBMPR1A-FLAG showed significantly reduced migration compared with control explants (Figure 2E), consistent with an autonomous role for BMP signaling on neural crest migration.

The results of these *in vivo* and *ex vivo* experiments could alternatively be explained by a reduction in neural crest cell count or could reflect a defect in delamination from the dorsal neural tube. To test these alternative hypotheses, we performed cell counting analysis and

found no significant difference in SOX9+ or SNAI2+ neural crest cells following dnBMPR1A-FLAG expression (Supplemental Figure 2). Further, successful EMT and delamination requires downregulation of Cadherin-6B (Coles et al., 2007; Schiffmacher et al., 2016; Taneyhill et al., 2007) and remodeling of the laminin-rich basement membrane (Hutchins and Bronner, 2019). By performing immunohistochemistry for these markers, we found comparable staining patterns between control and BMP-inhibited neural crest cells (Supplemental Figure 2, Figure 2F), suggesting that BMP signaling during neurulation is not required for EMT or delamination. Together, these results indicate that BMP signaling acts autonomously on cranial neural crest cells to control their migration in a manner independent of specification and delamination.

Identification of BMP-responsive genes during midbrain neural crest epithelial-to-mesenchymal transition

The observation that BMP signaling inhibition reduced migration of midbrain neural crest raised the question of which gene targets might be regulated by BMP signaling to facilitate cranial neural crest migration. To identify both direct and indirect targets of BMP signaling, we adopted a transcriptome profiling approach and examined changes in gene expression upon inhibition of BMP signaling during EMT (Figure 3A). Accordingly, we expressed control RFP or dnBMPR1A together with NC1.1m3::EGFP and incubated embryos until the onset of midbrain neural crest migration (8ss). Embryo heads were then dissociated into single-cell suspensions and EGFP-positive, BMP-inhibited neural crest cells were isolated by fluorescence-activated cell sorting. After preparation of cDNA libraries, we performed bulk RNA-sequencing and differential gene expression analysis to compare BMP-inhibited neural crest with RFP-expressing control cells (controls collected in concert with (Hutchins et al., 2021)).

The results show that dnBMPR1A-FLAG expression resulted in 42 down- and 42 up-regulated genes, using a fold change cutoff greater than 1.8 and a false discovery rate below 0.05 (Figure 3B, Supplemental Figure S3A). To discriminate whether these targets are specific to neural crest migration or reflect a defect in neural crest specification, we examined expression of canonical neural crest gene regulatory network (GRN) members (Martik and Bronner, 2017). The majority of bona fide neural crest specification markers, including *SOX10*, were not significantly disrupted by dnBMPR1A-FLAG electroporation (Supplemental Figure S3B). Further, *SNAI2*, *RHOB*, and *CDH6* (Cadherin-6B), each of which are implicated in neural crest EMT (Coles et al., 2007; Groysman et al., 2008; Liu and Jessell, 1998; Nieto et al., 1994; Schiffmacher et al., 2016; Taneyhill et al., 2007), were unaffected by BMP inhibition although another gene involved in neural crest EMT *ZEB2/SIP1* (Rogers et al., 2013) was altered. This indicates that BMP signaling regulates both known and novel candidate genes during neural crest EMT and this function is independent of overall neural crest specification.

Functional annotation of BMPR1A targets

We next performed functional annotation of the BMPR1A-responsive gene sets using PANTHER (Mi et al., 2019). Molecular functions assigned to these gene targets were most predominantly associated with transcriptional regulation, structural and cytoskeletal

function, and signal transduction (Figure 3D). These molecular functions are essential during EMT and cell migration; therefore, misregulation of these genes is likely responsible for reduction in neural crest migration following BMP inhibition. The most significantly downregulated targets of dnBMPR1A-FLAG, reflecting genes positively regulated by BMP signaling, included members of the *MSX*, *ID*, and *DLX* families of transcriptional regulators (e.g. *ID1-4*, *MSX1-2*, *DLX5*, Figure 3B, 3C), consistent with previous work documenting these as canonical BMP signaling targets during craniofacial development (Bonilla-Claudio et al., 2012; Graf et al., 2016; Levi et al., 2006; Miyazono and Miyazawa, 2003; Nie et al., 2006; Tríbulo et al., 2003).

Numerous genes were upregulated by dnBMPR1A-FLAG, reflecting genes that are likely suppressed by endogenous BMP signaling. The most dramatically upregulated target was *BMPR1A*, capturing our experimental overexpression of the dnBMPR1A-FLAG construct. Other notably upregulated targets include basic helix-loop-helix transcription factors belonging to the *HES* family (*HES6-2*, *HES5-3*, *HES5-1*), and *NHLH1* (Figure 3B, 3C). These genes are targets of Notch signaling and regulate neuronal proliferation and differentiation (Fior and Henrique, 2005; Vilas-Boas and Henrique, 2010). Ectopic upregulation of these genes in BMP-inhibited neural crest cells may reflect precocious activation of Notch signaling, suggesting that there is crosstalk between the BMP and Notch signaling pathways during early neural crest migration.

We also examined significantly enriched Gene Ontology (GO) Biological Processes (Carbon et al., 2019) in the down- and up-regulated gene sets (Figure 3D). We observed a significant enrichment in genes involved in “epithelial-to-mesenchymal transition”, “negative regulation of cell differentiation”, “establishment of cell polarity”, and “Rac protein signal transduction” in the downregulated gene set. As these processes include genes essential for normal EMT and cell migration, these results are consistent with the reduced midbrain neural crest migration we observed following BMP inhibition (Figure 2). Additionally, we observed enrichment of biological processes associated with lipid metabolism and in P-body assembly among downregulated genes, suggesting that BMP signaling regulates additional cellular physiologies that are emerging as novel regulators of neural crest EMT (Hutchins et al., 2020; Piacentino et al., 2020a). Conversely, the upregulated gene set showed biological processes including “neurogenesis”, “positive regulation of neuron projection development”, “negative regulation of cell migration”, “pharyngeal system development”, and “head development”. Together with the expression of Notch signaling targets and the role of Notch signaling in neuronal differentiation (Fior and Henrique, 2005; Vilas-Boas and Henrique, 2010), these results suggest that BMP signaling during neural crest EMT and migration suppresses premature differentiation into neurogenic fates. Together, this analysis provides novel insight into the role of BMP signaling during midbrain neural crest EMT.

Validation of BMPR1A-responsive transcriptional targets

To validate that transcriptional targets identified in our screen are indeed sensitive to BMP inhibition, we performed quantitative hybridization chain reaction (HCR) for a subset of BMP targets in dnBMPR1A-FLAG-electroporated embryos. We measured the mean fluorescence intensity within the midbrain neural crest domain to test for differential gene

expression *in vivo* (Figure 4). The results show significant downregulation of *ID2*, consistent with our RNA-seq results and with previous reports characterizing *ID2* as a target of BMP (Bonilla-Claudio et al., 2012; Miyazono and Miyazawa, 2003). Our transcriptome profiling identified both *HES6-2* and *APOD* as upregulated following BMP inhibition (Figure 3B, 3C), and HCR analysis showed a similar increase in expression of these genes (Figure 4). Finally, the neural crest specification marker *TFAP2B* was unaffected by dnBMPR1A-FLAG electroporation by both RNA-seq and by HCR analysis (Figure 4, Supplemental Figure 3B). These results validate that our transcriptome profiling successfully identified both down- and up-regulated targets of BMPR1A function and provides a valuable resource for deciphering how BMP signaling regulates cranial neural crest delamination and early migration.

Discussion

Here we examined the role of BMP signaling on neural crest EMT from the avian midbrain. Using fluorescent reporter constructs, we have identified a peak in BMP activity that coincides with neural crest delamination (Figure 1). Through BMP inhibition experiments, we found that BMP signaling is required for appropriate neural crest migration, independent of regulating specification and delamination (Figure 2, Supplemental Figure S2, Supplemental Figure S3). In the rostral hindbrain, neural crest migration speed and directionality is constrained by DAN-mediated BMP inhibition (McLennan et al., 2017). Since DAN expression is absent from the mesoderm adjacent to the midbrain (McLennan et al., 2017), lack of BMP inhibition may contribute to the unrestricted “fan”-like migration pattern of midbrain neural crest as compared to the confined streams observed in the more caudal hindbrain levels.

Using RNA sequencing we have identified and validated novel targets of BMP signaling during midbrain neural crest EMT and delamination (Figure 3). Among genes positively regulated by BMP signaling, we observed a loss of several genes shown to promote cell migration in other contexts (e.g. *ID1* (Li et al., 2017), *ID2* (Coma et al., 2010), *RABIF* (Moissoglu et al., 2020), *UNC119B* (Liu et al., 2018), *PLK1* (Yan et al., 2018), *RIOX1* (Nishizawa et al., 2017), and *METRNL* (Jørgensen et al., 2012)). Thus, loss of these genes likely reflects the mechanisms by which BMP signaling promotes early cranial neural crest migration. Further, these results provide interesting insights into potential crosstalk between different signaling pathways during early craniofacial development. The transcriptional targets of the Wnt and BMP signaling pathways in delaminating cranial neural crest cells are largely non-overlapping, despite evidence that BMP suppresses expression of the Wnt antagonist *DRAXIN* (Supplemental Figure 3), and Wnt upregulates *BMP4* (Hutchins et al., 2021). This suggests that Wnt and BMP signaling play parallel regulatory roles during cranial neural crest delamination; this differs from the consecutive functions of BMP and Wnt signaling during trunk neural crest EMT (Burstyn-Cohen et al., 2004; Kalcheim, 2015).

Our results also provide new insight into the differences between neural crest cells from different axial levels. In the cranial neural crest, Wnt but not BMP signaling regulates expression of *RHOB* (Supplemental Figure 3 and (Hutchins et al., 2021), while this relationship is reversed in trunk neural crest cells where BMP, but not Wnt, regulates *RHOB*

(Liu and Jessell, 1998; Taneyhill and Bronner-Fraser, 2005). This illustrates the importance of identifying the specific transcriptional targets of different signaling pathways in the cranial neural crest to better prevent atypical craniofacial development.

Of the few overlapping targets between BMP and Wnt signaling, the most notable include Notch-dependent targets involved in neuronal differentiation (Fior and Henrique, 2005; Vilas-Boas and Henrique, 2010). While BMP suppresses expression of *HES6-3*, *HES5-3*, and *HES5-1*, Wnt signaling positively regulates *HES5-3*, *HES5-2*, and *HES5-1* (Hutchins et al., 2021). This suggests that Wnt signaling may play a role in activating the Notch pathway, while BMP suppresses its activity. The function of these pathways together may act to segregate the midbrain neural crest into different subpopulations: BMP suppressing neurogenic fates to maintain chondrogenic potential, with Wnt activating Notch signaling to support neurogenesis within a separate subpopulation. Consistent with the idea of these neural crest subpopulations, we observed a scattered expression of the genes *HES6-2* and *APOD* in BMP-inhibited neural crest, which resembles the “salt-and-pepper” expression patterns of many Notch-responsive targets (Chrysostomou et al., 2020; Fior and Henrique, 2005; Pajaniappan et al., 2011; Vilas-Boas and Henrique, 2010).

Together, our results demonstrate a requirement for BMP signaling in delaminating midbrain neural crest and identify novel transcriptional targets of BMP signaling during this process. These results provide insight into the potential for crosstalk between the BMP, Wnt, and Notch signaling pathways during neural crest migration. This study provides a valuable resource for future experiments in dissecting the mechanisms regulated by BMP signaling during early craniofacial development.

Materials and Methods

Chick embryos and electroporations

Chicken embryos were harvested from fertilized eggs obtained from local sources (Sunstate Ranch, Sylmar, CA). Embryos were electroporated *ex ovo* and cultured as previously described (Piacentino and Bronner, 2018). BRE::H2B-d2EGFP, 2a-RFP, and dnBMPR1A-FLAG constructs were each electroporated at 2.5 μg/μl and *FoxD3* NC1.1m3::EGFP (Simões-Costa et al., 2012) was electroporated at 3 μg/μl. Only embryos with high electroporation efficiency as determined by fluorescent protein expression were included in analyses.

Construct design and cloning

DNA constructs were produced by PCR reactions with AccuPrime high-fidelity DNA polymerase (ThermoFisher) followed by standard restriction enzyme digestion and ligation (NEB); primer sequences and source constructs are presented in the Key Resources Table. In each case, a 5’ Kozak consensus sequence was introduced to promote translation, and each construct was verified by sequencing before use. BRE::H2B-d2EGFP was produced to drive destabilized, nuclear EGFP under control of BMP activity by amplifying H2B-d2EGFP from TCF/Lef::H2B-d2EGFP (Piacentino et al., 2020a) with AscI cut sites using “H2B AscI FWD” and “d2EGFP AscI REV”. The BRE vector sequence (le Dréau et al., 2012) was

amplified with AscI cut sites using “BRE AscI FWD” and “BRE AscI REV”. Products were then digested with AscI and ligated together. pCAG::2a-RFP drives RFP expression immediately downstream a self-cleaving 2a peptide. RFP was amplified from pCI::H2B-RFP (Betancur et al., 2010), and the 2a sequence was added by sequential amplification with “2a-RFP FWD 1”, then “2a-RFP FWD 2”, then “2a-RFP FWD 3 ClaI” primers, each with “RFP stop REV NotI”. The resulting 2a-RFP sequence was then ligated into pCI::H2B-RFP between the ClaI and NotI cut sites. To produce pCAG::dnBMPR1A-FLAG, C-terminal truncated BMPR1A was amplified and the FLAG tag was added using “BMPR1A ATG XhoI FWD” and “dnBMPR1A-FLAG REV ClaI”, then digested and ligated into pCAG::2a-RFP between XhoI and ClaI cut sites.

Immunohistochemistry and hybridization chain reaction

Embryos were fixed and immuostained in whole mount as previously described (Piacentino and Bronner, 2018). Primary antibodies employed in this study include mouse IgG1 anti-PAX7 (1:10; DSHB #PAX7), mouse IgG1 anti-Cadherin-6B (1:5; DSHB #CCD6B-1), rabbit anti-SNAI2 (1:500; Cell Signaling Technologies #9585), rabbit anti-SOX9 (1:1000; Sigma-Aldrich #AB5535), rabbit anti-laminin (1:500; Sigma-Aldrich #L9393), mouse IgG1 anti-FLAG (1:500; Sigma-Aldrich #F1804), rabbit anti-phosphoSMAD1/5/8 (1:100; Cell Signaling Technologies #13820), goat anti-GFP (1:500; Rockland #600-101-215M), and rabbit anti-RFP (1:500; MBL #PM005). Primary antibodies were detected by Alexa Fluor 488-, 568-, or 647-conjugated donkey secondary antibodies (1:500; Molecular Probes). For transverse sectioning, immunostained embryos were postfixed for 2 hours at room temperature in 4% PFA in phosphate buffer, washed with PBS, then incubated in 5% sucrose for 15 minutes at room temperature, in 15% sucrose at 4°C overnight, in 7.5% gelatin overnight at 39°C, then flash-frozen in liquid nitrogen and cryosectioned at a thickness of 18 μm. Hybridization Chain Reaction reagents were purchased from Molecular Technologies, and experiments followed manufacturer’s instructions (Choi et al., 2018). Probe sets were designed against *TFAP2B* (B7 initiator, (Gandhi et al., 2020)), *Id2* (B6), *HES6-2* (B6), *APOD* (B5), and detected using appropriate Alexa488 and Alexa647 amplifier hairpins.

Cranial neural crest explants

For explant experiments, polymer coverslip bottom imaging chambers (ibidi #80821) were coated with 25 μg/mL fibronectin (Millipore Sigma #FC010) in PBS and incubated at 37°C for 1 hour after which fibronectin was aspirated and allowed to dry. Embryos were electroporated at gastrulation and incubated until premigratory neural crest stages (5 somite stage), at which point 2a-RFP- and dnBMPR1A-electroporated dorsal neural tubes were explanted from the midbrain axial level and cultured in an imaging chamber containing DMEM supplemented with 10% Fetal Bovine Serum, 1% Penicillin/Streptomycin, and 1% L-Glutamate, and cultured at 37°C with 5% CO_2. Explants were allowed to adhere to the fibronectin-coated dish, then imaged for bright field and RFP fluorescence at 2 and 24 hours post explant.

RNA Seq Analysis

Embryos electroporated for RNA sequencing analysis were dissected, dissociated, and EGFP-positive cells were isolated by fluorescence activated cell sorting at the Caltech Flow

Cytometry Cell Sorting Facility as previously described (Hutchins et al., 2021). We prepared cDNA libraries from >1000 GFP-positive cells per replicate using SMART-Seq v4 Ultra Low Input cDNA Kit (Takara Bio) following manufacturer's instructions. Libraries were then sequenced at the Caltech Millard and Muriel Jacobs Genetics and Genomics Laboratory. 35 million 50bp single-end reads were collected on an Illumina HiSeq machine for each of two biological replicates of the dnBMPR1A-FLAG-expressing cranial neural crest cells. For differential analysis, RFP control (Hutchins et al., 2021) and BMP-inhibited reads were trimmed using Cutadapt (Martin, 2011), aligned to the GRCg6a chicken genome using BowTie2 (Langmead and Salzberg, 2012), transcripts were counted using FeatureCounts (Liao et al., 2014), and differential expression was determined using DESeq2 (Love et al., 2014). Resulting gene lists were analyzed using functional annotations in PANTHER (Mi et al., 2019).

Microscopy, image, and statistical analysis

Imaging of whole mount embryos, transverse sections, and explant experiments was performed on a Zeiss Imager.M2 with an ApoTome.2 module, and whole mount imaging of HCR experiments was performed on a Zeiss LSM880 confocal microscope. All transverse section images and panels in Figure 4A display maximum intensity projections of Z-stacks, while the remaining whole mount images display wide-field views. Image analysis and display preparation was performed using Fiji (Schindelin et al., 2012). To measure BMP activity single optical sections were subjected to median filtering, thresholded using the Max Entropy method in the Auto Threshold tool, and size filtered to assign regions of interest corresponding to individual neural crest nuclei of greater than 15.0 μm^2. BRE::H2B-d2EGFP and RFP channel intensity was measured from each nucleus, and corrected total cellular fluorescence was calculated and normalized as previously described (Piacentino and Bronner, 2018). Neural crest migration area and relative HCR signal intensity was determined by manually drawing regions of interest surrounding the neural crest along a 400 μm length of the midbrain and measuring the area or mean fluorescence intensity, respectively. Explant migration area was measured manually in Fiji from brightfield images collected at 2 and 24 hours post explant (hpe), and explant fold area change was calculated by dividing 24 hpe area by 2 hpe area. Cell counting was performed on transverse sections in Fiji as previously described (Piacentino and Bronner, 2018). All data analyses and plotting were performed in Python (v3.7.6) using the packages listed in the Key Resources Table. All statistical tests are described in the corresponding figure legends, and source data and analysis code are available at https://github.com/mpiacentino/2021-Transcriptome-profiling-reveals-BMP-target-genes-during-midbrain-neural-crest-delamination.

Supplementary Material

Refer to Web version on PubMed Central for supplementary material.

Acknowledgments

We would like to thank Megan Martik and Shashank Gandhi for valuable discussion on experiment design and analysis, and Gabriel da Silva Pescador for technical support. We thank Elisa Martí for sharing reagents, Patrick Cannon and Rochelle Diamond at the Caltech Flow Cytometry Cell Sorting Facility for cell sorting, Igor Antoshechkin of the Caltech Millard and Muriel Jacobs Genetics and Genomics Laboratory for library sequencing,

and the Beckman Institute Biological Imaging Facility for microscopy support. Funding for this work comes from the National Institutes of Health grants K99DE029240 to M.L.P., K99DE028592 to E.J.H, R01DE027538 and R01DE027568 to M.E.B.

References

Andrée B, Duprez D, Vorbusch B, Arnold HH, Brand T, 1998. BMP-2 induces ectopic expression of cardiac lineage markers and interferes with somite formation in chicken embryos. Mechanisms of Development 70, 119–131. 10.1016/S0925-4773(97)00186-X [PubMed: 9510029]

Araya C, Mayor R, Kuriyama S, Steventon B, Linker C, 2009. Differential requirements of BMP and Wnt signalling during gastrulation and neurulation define two steps in neural crest induction. Development 136, 771–779. 10.1242/dev.029017 [PubMed: 19176585]

Betancur P, Bronner-Fraser M, Sauka-Spengler T, 2010. Genomic code for Sox10 activation reveals a key regulatory enhancer for cranial neural crest . Proceedings of the National Academy of Sciences 107, 3570–3575. 10.1073/pnas.0906596107

Bois JS (2020). justinbois/iqplot: 0.1.6.

Bokeh Development Team (2018). Bokeh: Python library for interactive visualization.

Bonilla-Claudio M, Wang J, Bai Y, Klysik E, Selever J, Martin JF, 2012. Bmp signaling regulates a dose-dependent transcriptional program to control facial skeletal development. Development 139, 709–719. 10.1242/dev.073197 [PubMed: 22219353]

Bothe I, Tenin G, Oseni A, Dietrich S, 2011. Dynamic control of head mesoderm patterning. Development 138, 2807–2821. 10.1242/dev.062737 [PubMed: 21652653]

Burstyn-Cohen T, Stanleigh J, Sela-Donenfeld D, Kalcheim C, 2004. Canonical Wnt activity regulates trunk neural crest delamination linking BMP/noggin signaling with G1/S transition. Development 131, 5327–5339. 10.1242/dev.01424 [PubMed: 15456730]

Carbon S, Douglass E, Dunn N, Good B, Harris NL, Lewis SE, Mungall CJ, Basu S, Chisholm RL, Dodson RJ, Hartline E, Fey P, Thomas PD, Albou LP, Ebert D, Kesling MJ, Mi H, Muruganujan A, Huang X, Poudel S, Mushayahama T, Hu JC, LaBonte SA, Siegele DA, Antonazzo G, Attrill H, Brown NH, Fexova S, Garapati P, Jones TEM, Marygold SJ, Millburn GH, Rey AJ, Trovisco V, dos Santos G, Emmert DB, Falls K, Zhou P, Goodman JL, Strelets VB, Thurmond J, Courtot M, Osumi DS, Parkinson H, Roncaglia P, Acencio ML, Kuiper M, Lreid A, Logie C, Lovering RC, Huntley RP, Denny P, Campbell NH, Kramarz B, Acquaah V, Ahmad SH, Chen H, Rawson JH, Chibucos MC, Giglio M, Nadendla S, Tauber R, Duesbury MJ, Del NT, Meldal BHM, Perfetto L, Porras P, Orchard S, Shrivastava A, Xie Z, Chang HY, Finn RD, Mitchell AL, Rawlings ND, Richardson L, Sangrador-Vegas A, Blake JA, Christie KR, Dolan ME, Drabkin HJ, Hill DP, Ni L, Sitnikov D, Harris MA, Oliver SG, Rutherford K, Wood V, Hayles J, Bahler J, Lock A, Bolton ER, de Pons J, Dwinell M, Hayman GT, Laulederkind SJF, Shimoyama M, Tutaj M, Wang SJ, D'Eustachio P, Matthews L, Balhoff JP, Aleksander SA, Binkley G, Dunn BL, Cherry JM, Engel SR, Gondwe F, Karra K, MacPherson KA, Miyasato SR, Nash RS, Ng PC, Sheppard TK, Shrivatsav Vp A, Simison M, Skrzypek MS, Weng S, Wong ED, Feuermann M, Gaudet P, Bakker E, Berardini TZ, Reiser L, Subramaniam S, Huala E, Arighi C, Auchincloss A, Axelsen K, Argoud GP, Bateman A, Bely B, Blatter MC, Boutet E, Breuza L, Bridge A, Britto R, Bye-A-Jee H, Casals-Casas C, Coudert E, Estreicher A, Famiglietti L, Garmiri P, Georghiou G, Gos A, Gruaz-Gumowski N, Hatton-Ellis E, Hinz U, Hulo C, Ignatchenko A, Jungo F, Keller G, Laiho K, Lemercier P, Lieberherr D, Lussi Y, Mac-Dougall A, Magrane M, Martin MJ, Masson P, Natale DA, Hyka NN, Pedruzzi I, Pichler K, Poux S, Rivoire C, Rodriguez-Lopez M, Sawford T, Speretta E, Shypitsyna A, Stutz A, Sundaram S, Tognolli M, Tyagi N, Warner K, Zaru R, Wu C, Chan J, Cho J, Gao S, Grove C, Harrison MC, Howe K, Lee R, Mendel J, Muller HM, Raciti D, van Auken K, Berriman M, Stein L, Sternberg PW, Howe D, Toro S, Westerfield M, 2019. The Gene Ontology Resource: 20 years and still GOing strong. Nucleic Acids Research 47, D330–D338. 10.1093/nar/gky1055 [PubMed: 30395331]

Cheah KSE, Yan CH, So H, Chau BKH, Briscoe J, Ng A, Chan A, Liu JAJ, Wu M-H, Cheung M, 2013. Phosphorylation of Sox9 is required for neural crest delamination and is regulated downstream of BMP and canonical Wnt signaling. Proceedings of the National Academy of Sciences 110, 2882–2887. 10.1073/pnas.1211747110

Choi HMT, Schwarzkopf M, Fornace ME, Acharya A, Artavanis G, Stegmaier J, Cunha A, Pierce NA, 2018. Third-generation in situ hybridization chain reaction: multiplexed, quantitative, sensitive, versatile, robust. Development (Cambridge, England) 145. 10.1242/dev.165753

Chrysostomou E, Zhou L, Darcy YL, Graves KA, Doetzlhofer A, Cox BC, 2020. The notch ligand jagged1 is required for the formation, maintenance, and survival of Hensen's cells in the mouse cochlea. Journal of Neuroscience 40, 9401–9413. 10.1523/JNEUROSCI.1192-20.2020 [PubMed: 33127852]

Coles EG, Taneyhill LA, Bronner-Fraser M, 2007. A critical role for Cadherin6B in regulating avian neural crest emigration. Developmental Biology 312, 533–544. 10.1016/j.ydbio.2007.09.056 [PubMed: 17991460]

Coma S, Amin DN, Shimizu A, Lasorella A, Iavarone A, Klagsbrun M, 2010. Id2 promotes tumor cell migration and invasion through transcriptional repression of semaphorin 3F. Cancer Research 70, 3823–3832. 10.1158/0008-5472.CAN-09-3048 [PubMed: 20388805]

Couly GF, Coltey PM, le Douarin NM, 1993. The triple origin of skull in higher vertebrates: A study in quail-chick chimeras. Development 117.

Das A, Crump JG, 2012. Bmps and Id2a act upstream of twist1 to restrict ectomesenchyme potential of the cranial neural crest. PLoS Genetics 8. 10.1371/journal.pgen.1002710

Dudas M, Sridurongrit S, Nagy A, Okazaki K, Kaartinen V, 2004. Craniofacial defects in mice lacking BMP type I receptor Alk2 in neural crest cells. Mechanisms of Development 121, 173–182. 10.1016/j.mod.2003.12.003 [PubMed: 15037318]

Fior R, Henrique D, 2005. A novel hes5/hes6 circuitry of negative regulation controls Notch activity during neurogenesis. Developmental Biology 281, 318–333. 10.1016/j.ydbio.2005.03.017 [PubMed: 15893982]

Gandhi S, Bronner ME, 2018. Insights into neural crest development from studies of avian embryos. International Journal of Developmental Biology 62, 179–190. 10.1387/ijdb.180038sg

Gandhi S, Hutchins EJ, Maruszko K, Park JH, Thomson M, Bronner ME, 2020. Bimodal function of chromatin remodeler hmga1 in neural crest induction and wnt-dependent emigration. eLife 9, 1–62. 10.7554/ELIFE.57779

Goldstein AM, Brewer KC, Doyle AM, Nagy N, Roberts DJ, 2005. BMP signaling is necessary for neural crest cell migration and ganglion formation in the enteric nervous system. Mechanisms of Development 122, 821–833. 10.1016/j.mod.2005.03.003 [PubMed: 15905074]

Graf D, Malik Z, Hayano S, Mishina Y, 2016. Common mechanisms in development and disease: BMP signaling in craniofacial development. Cytokine and Growth Factor Reviews. 10.1016/j.cytogfr.2015.11.004

Graham A, Francis-West P, Brickell P, Lumsden A, FRANCISWEST P, Brickell P, Lumsden A, 1994. The Signaling Molecule Bmp4 Mediates Apoptosis in the Rhombencephalic Neural Crest. Nature 372, 684–686. 10.1038/372684a0 [PubMed: 7990961]

Groysman M, Shoval I, Kalcheim C, 2008. A negative modulatory role for rho and rho-associated kinase signaling in delamination of neural crest cells. Neural Development 3, 1–22. 10.1186/1749-8104-3-27

Hsu S-Y, Chou T-Y, Ouyang P, Shih H-Y, Cheng Y-C, Lin S-J, Chiang M-C, 2016. Bmp5 Regulates Neural Crest Cell Survival and Proliferation via Two Different Signaling Pathways. Stem Cells 35, 1003–1014. 10.1002/stem.2533 [PubMed: 27790787]

Hutchins EJ, Bronner ME, 2019. Draxin alters laminin organization during basement membrane remodeling to control cranial neural crest EMT. Developmental Biology 446, 151–158. 10.1016/j.ydbio.2018.12.021 [PubMed: 30579765]

Hutchins EJ, Kunttas E, Piacentino ML, Howard AGA, Bronner ME, Uribe RA, 2018. Migration and diversification of the vagal neural crest. Developmental Biology 444, S98–S109. 10.1016/j.ydbio.2018.07.004 [PubMed: 29981692]

Hutchins EJ, Piacentino ML, Bronner ME, 2021. Transcriptomic Identification of Draxin-Responsive Targets During Cranial Neural Crest EMT. Frontiers in Physiology 12. 10.3389/fphys.2021.624037

Hutchins EJ, Piacentino ML, Bronner ME, 2020. P-bodies are sites of rapid RNA decay during the neural crest epithelial — mesenchymal transition. bioRxiv 1–15.

Ihaka R, and Gentleman R (1996). R: A Language for Data Analysis and Graphics. Journal of Computational and Graphical Statistics 5.

Jørgensen JR, Fransson A, Fjord-Larsen L, Thompson LH, Houchins JP, Andrade N, Torp M, Kalkkinen N, Andersson E, Lindvall O, Ulfendahl M, Brunak S, Johansen TE, Wahlberg LU, 2012. Cometin is a novel neurotrophic factor that promotes neurite outgrowth and neuroblast migration in vitro and supports survival of spiral ganglion neurons in vivo. Experimental Neurology 233, 172–181. 10.1016/j.expneurol.2011.09.027 [PubMed: 21985865]

Kalcheim C, 2015. Epithelial–Mesenchymal Transitions during Neural Crest and Somite Development. Journal of Clinical Medicine 5, 1. 10.3390/jcm5010001

Kanzler B, Foreman RK, Labosky PA, Mallo M, 2000. BMP signaling is essential for development of skeletogenic and neurogenic cranial neural crest. Development 127, 1095–1104. [PubMed: 10662648]

Komatsu Y, Yu PB, Kamiya N, Pan H, Fukuda T, Scott GJ, Ray MK, Yamamura KI, Mishina Y, 2013a. Augmentation of Smad-dependent BMP signaling in neural crest cells causes craniosynostosis in mice. Journal of Bone and Mineral Research 28, 1422–1433. 10.1002/jbmr.1857 [PubMed: 23281127]

Komatsu Y, Yu PB, Kamiya N, Pan H, Fukuda T, Scott GJ, Ray MK, Yamamura KI, Mishina Y, 2013b. Augmentation of Smad-dependent BMP signaling in neural crest cells causes craniosynostosis in mice. Journal of Bone and Mineral Research 28, 1422–1433. 10.1002/jbmr.1857 [PubMed: 23281127]

Langmead B, Salzberg SL, 2012. Fast gapped-read alignment with Bowtie 2. Nature Methods 9, 357–359. 10.1038/nmeth.1923 [PubMed: 22388286]

le Douarin NM, Creuzet S, Couly G, Dupin E, 2004. Neural crest cell plasticity and its limits. Development. 10.1242/dev.01350

le Dréau G, Garcia-Campmany L, Angeles Rabadán M, Ferronha T, Tozer S, Briscoe J, Martí E, 2012. Canonical BMP7 activity is required for the generation of discrete neuronal populations in the dorsal spinal cord. Development 139, 259–268. 10.1242/dev.074948 [PubMed: 22159578]

Levi G, Mantero S, Barbieri O, Cantatore D, Paleari L, Beverdam A, Genova F, Robert B, Merlo GR, 2006. Msx1 and Dlx5 act independently in development of craniofacial skeleton, but converge on the regulation of Bmp signaling in palate formation. Mechanisms of Development 123, 3–16. 10.1016/j.mod.2005.10.007 [PubMed: 16330189]

Li J, Li Y, Wang B, Ma Y, Chen P, 2017. Id-1 promotes migration and invasion of non-small cell lung cancer cells through activating NF-κB signaling pathway. Journal of Biomedical Science 24, 95. 10.1186/s12929-017-0400-6 [PubMed: 29233161]

Liao Y, Smyth GK, Shi W, 2014. FeatureCounts: An efficient general purpose program for assigning sequence reads to genomic features. Bioinformatics 30, 923–930. 10.1093/bioinformatics/btt656 [PubMed: 24227677]

Liu J, Jessell TM, 1998. A role for rhoB in the delamination of neural crest cells from the dorsal neural tube.

Liu Z, Zhang Y, Xu Z, 2018. UNC119 promotes the growth and migration of hepatocellu-lar carcinoma via Wnt/β-catenin and TGF-β/EMT signaling pathways. JBUON 23, 185–192. [PubMed: 29552781]

Love MI, Huber W, Anders S, 2014. Moderated estimation of fold change and dispersion for RNA-seq data with DESeq2. Genome Biology 15, 1–21. 10.1186/s13059-014-0550-8

Maéno M, Ong RC, Suzuki A, Ueno N, Kung HF, 1994. A truncated bone morphogenetic protein 4 receptor alters the fate of ventral mesoderm to dorsal mesoderm: Roles of animal pole tissue in the development of ventral mesoderm. Proceedings of the National Academy of Sciences of the United States of America 91, 10260–10264. 10.1073/pnas.91.22.10260 [PubMed: 7937937]

Marchant L, Linker C, Ruiz P, Guerrero N, Mayor R, 1998. The inductive properties of mesoderm suggest that the neural crest cells are specified by a BMP gradient. Developmental Biology 198, 319–329. 10.1006/dbio.1998.8902 [PubMed: 9659936]

Martik ML, Bronner ME, 2017. Regulatory Logic Underlying Diversification of the Neural Crest. Trends in Genetics 33, 715–727. 10.1016/j.tig.2017.07.015 [PubMed: 28851604]

Martin M, 2011. Cutadapt removes adapter sequences from high-throughput sequencing reads. EMBnet.journal 17, 10. 10.14806/ej.17.1.200

McKinney W, and Team PD (2015). Pandas - Powerful Python Data Analysis Toolkit. Pandas - Powerful Python Data Analysis Toolkit.

McLennan R, Bailey CM, Schumacher LJ, Teddy JM, Morrison JA, Kasemeier-Kulesa JC, Wolfe LA, Gogol MM, Baker RE, Maini PK, Kulesa PM, 2017. DAN (NBL1) promotes collective neural crest migration by restraining uncontrolled invasion. Journal of Cell Biology 216, 3339–3354. 10.1083/jcb.201612169

Mi H, Muruganujan A, Ebert D, Huang X, Thomas PD, 2019. PANTHER version 14: More genomes, a new PANTHER GO-slim and improvements in enrichment analysis tools. Nucleic Acids Research 47. 10.1093/nar/gky1038

Miyazono K, Kamiya Y, Morikawa M, 2010. Bone morphogenetic protein receptors and signal transduction. Journal of Biochemistry. 10.1093/jb/mvp148

Miyazono K, Miyazawa K, 2003. Id: A Target of BMP Signaling. Science Signaling 2002, pe40–pe40. 10.1126/stke.2002.151.pe40

Moissoglu K, Stueland M, Gasparski AN, Wang T, Jenkins LM, Hastings ML, Mili S, 2020. RNA localization and co-translational interactions control RAB 13 GTP ase function and cell migration . The EMBO Journal 39. 10.15252/embj.2020104958

Nie X, Luukko K, Kettunen P, 2006. BMP signalling in craniofacial development. The International Journal of Developmental Biology 50, 511–521. 10.1387/ijdb.052101xn [PubMed: 16741866]

Nieto MA, Sargent MG, Wilkinson DG, Cooke J, 1994. Control of cell behavior during vertebrate development by Slug, a zinc finger gene. Science 264, 835–839. 10.1126/science.7513443 [PubMed: 7513443]

Nishizawa Y, Nishida N, Konno M, Kawamoto K, Asai A, Koseki J, Takahashi H, Haraguchi N, Nishimura J, Hata T, Matsuda C, Mizushima T, Satoh T, Doki Y, Mori M, Ishii H, 2017. Clinical Significance of Histone Demethylase NO66 in Invasive Colorectal Cancer. Annals of Surgical Oncology 24, 841–849. 10.1245/s10434-016-5395-9 [PubMed: 27473587]

Noden DM, 1983. The role of the neural crest in patterning of avian cranial skeletal, connective, and muscle tissues. Developmental Biology 96, 144–165. 10.1016/0012-1606(83)90318–4 [PubMed: 6825950]

Pajaniappan M, Glober NK, Kennard S, Liu H, Zhao N, Lilly B, 2011. Endothelial cells downregulate apolipoprotein D expression in mural cells through paracrine secretion and Notch signaling. American Journal of Physiology - Heart and Circulatory Physiology 301, H784–H793. 10.1152/ajpheart.00116.2011 [PubMed: 21705670]

Park K-S, Gumbiner BM, 2010. Cadherin 6B induces BMP signaling and de-epithelialization during the epithelial mesenchymal transition of the neural crest. Development 137, 2691–2701. 10.1242/dev.050096 [PubMed: 20610481]

Pegge J, Tatsinkam AJ, Rider CC, Bell E, 2019. Heparan sulfate proteoglycans regulate BMP signalling during neural crest induction. Developmental Biology. 10.1016/j.ydbio.2019.12.015

Piacentino ML, Bronner ME, 2018. Intracellular attenuation of BMP signaling via CKIP-1/Smurf1 is essential during neural crest induction. PLoS Biology 16, 1–25. 10.1371/journal.pbio.2004425

Piacentino ML, Hutchins EJ, Andrews CJ, Bronner ME, 2020a. Temporal changes in plasma membrane lipid content induce endocytosis to regulate developmental epithelial-to-mesenchymal transition. bioRxiv. 10.1101/2020.10.18.344523

Piacentino ML, Li Y, Bronner ME, 2020b. Epithelial-to-mesenchymal transition and different migration strategies as viewed from the neural crest. Current Opinion in Cell Biology 66, 43–50. 10.1016/j.ceb.2020.05.001 [PubMed: 32531659]

Racine JS (2012). RSTUDIO: A platform-independent IDE for R and sweave. Journal of Applied Econometrics 27.

Rogers CD, Saxena A, Bronner ME, 2013. Sip1 mediates an E-cadherin-to-N-cadherin switch during cranial neural crest EMT. Journal of Cell Biology 203, 835–847. 10.1083/jcb.201305050

Schiffmacher AT, Xie V, Taneyhill LA, 2016. Cadherin-6B proteolysis promotes the neural crest cell epithelial-to-mesenchymal transition through transcriptional regulation. Journal of Cell Biology 215, 735–747. 10.1083/jcb.201604006

Schindelin J, Arganda-Carreras I, Frise E, Kaynig V, Longair M, Pietzsch T, Preibisch S, Rueden C, Saalfeld S, Schmid B, Tinevez JY, White DJ, Hartenstein V, Eliceiri K, Tomancak P, Cardona A, 2012. Fiji: An open-source platform for biological-image analysis. Nature Methods 9, 676–682. 10.1038/nmeth.2019 [PubMed: 22743772]

Schumacher JA, Hashiguchi M, Nguyen VH, Mullins MC, 2011. An intermediate level of bmp signaling directly specifies cranial neural crest progenitor cells in zebrafish. PLoS ONE 6. 10.1371/journal.pone.0027403

Sela-Donenfeld D, Kalcheim C, 2000. Inhibition of noggin expression in the dorsal neural tube by somitogenesis: a mechanism for coordinating the timing of neural crest emigration. Development (Cambridge, England) 127, 4845–54.

Sela-Donenfeld D, Kalcheim C, 1999. Regulation of the onset of neural crest migration by coordinated activity of BMP4 and Noggin in the dorsal neural tube. Development (Cambridge, England) 126, 4749–62.

Siismets EM, Hatch NE, 2020. Cranial neural crest cells and their role in the pathogenesis of craniofacial anomalies and coronal craniosynostosis. Journal of Developmental Biology. 10.3390/JDB8030018

Simoes-Costa M, Bronner ME, 2016. Reprogramming of avian neural crest axial identity and cell fate. Science 352, 1570–3. 10.1126/science.aaf2729 [PubMed: 27339986]

Simões-Costa MS, McKeown SJ, Tan-Cabugao J, Sauka-Spengler T, Bronner ME, 2012. Dynamic and Differential Regulation of Stem Cell Factor FoxD3 in the Neural Crest Is Encrypted in the Genome. PLoS Genetics 8, e1003142. 10.1371/journal.pgen.1003142 [PubMed: 23284303]

Stevens J-L, Rudiger P, and Bednar J (2015). HoloViews: Building Complex Visualizations Easily for Reproducible Science. In Proceedings of the 14th Python in Science Conference, p.

Streit A, Stern CD, 1999. Establishment and maintenance of the border of the neural plate in the chick: Involvement of FGF and BMP activity. Mechanisms of Development 82, 51–66. 10.1016/S0925-4773(99)00013-1 [PubMed: 10354471]

Suzuki A, Thies RS, Yamaji N, Song JJ, Wozney JM, Murakami K, Ueno N, 1994. A truncated bone morphogenetic protein receptor affects dorsal-ventral patterning in the early Xenopus embryo. Proceedings of the National Academy of Sciences of the United States of America 91, 10255–10259. 10.1073/pnas.91.22.10255 [PubMed: 7937936]

Taneyhill LA, Bronner-Fraser M, 2005. Dynamic alterations in gene expression, after Wnt-mediated induction of avian neural crest. Molecular Biology of the Cell 16. 10.1091/mbc.E05-03-0210

Taneyhill LA, Coles EG, Bronner-Fraser M, 2007. Snail2 directly represses cadherin6B during epithelial-to-mesenchymal transitions of the neural crest. Development 134, 1481–1490. 10.1242/dev.02834 [PubMed: 17344227]

Terpilowski M (2019). scikit-posthocs: Pairwise multiple comparison tests in Python. Journal of Open Source Software 4, 1169.

Theveneau E, Mayor R, 2012. Neural crest delamination and migration: From epithelium-to-mesenchyme transition to collective cell migration. Developmental Biology 366, 34–54. 10.1016/j.ydbio.2011.12.041 [PubMed: 22261150]

Tríbulo C, Aybar MJ, Nguyen VH, Mullins MC, Mayor R, 2003. Regulation of Msx genes by a Bmp gradient is essential for neural crest specification. Development 130, 6441–6452. 10.1242/dev.00878 [PubMed: 14627721]

van der Walt S, Colbert SC, and Varoquaux G (2011). The NumPy array: A structure for efficient numerical computation. Computing in Science and Engineering 13.

van Rossum G, and Drake FL (2009). Python 3 Reference Manual.

Vega-Lopez GA, Cerrizuela S, Tribulo C, Aybar MJ, 2018. Neurocristopathies: New insights 150 years after the neural crest discovery. Developmental Biology 444, 1–34. 10.1016/j.ydbio.2018.05.013 [PubMed: 30266259]

Vilas-Boas F, Henrique D, 2010. HES6–1 and HES6–2 function through different mechanisms during neuronal differentiation. PLoS ONE 5. 10.1371/journal.pone.0015459

Virtanen P, Gommers R, Oliphant TE, Haberland M, Reddy T, Cournapeau D, Burovski E, Peterson P, Weckesser W, Bright J, et al. (2020). SciPy 1.0: fundamental algorithms for scientific computing in Python. Nature Methods 17.

Waskom M (2012). Seaborn: Statistical Data Visualization.

Williams RM, Candido-Ferreira I, Repapi E, Gavriouchkina D, Senanayake U, Ling ITC, Telenius J, Taylor S, Hughes J, Sauka-Spengler T, 2019. Reconstruction of the Global Neural Crest Gene Regulatory Network In Vivo. Developmental Cell 51, 255–276.e7. 10.1016/j.devcel.2019.10.003 [PubMed: 31639368]

Wu MY, Ramel MC, Howell M, Hill CS, 2011. SNW1 is a critical regulator of spatial BMP activity, neural plate border formation, and neural crest specification in vertebrate embryos. PLoS Biology 9. 10.1371/journal.pbio.1000593

Yan W, Yu H, Li W, Li F, Wang S, Yu N, Jiang Q, 2018. Plk1 promotes the migration of human lung adenocarcinoma epithelial cells via STAT3 signaling. Oncology Letters 16, 6801–6807. 10.3892/ol.2018.9437 [PubMed: 30405824]

Yang J, Wedlich D, Severson C, Shi J, Klymkowsky MW, 2011. Snail2 controls mesodermal BMP/Wnt induction of neural crest. Development 138, 3135–3145. 10.1242/dev.064394 [PubMed: 21715424]

Highlights

1. BMP activity peaks in midbrain neural crest cells during delamination
2. BMP signaling is required for cranial neural crest migration
3. RNA Seq identifies novel BMP targets during cranial neural crest delamination

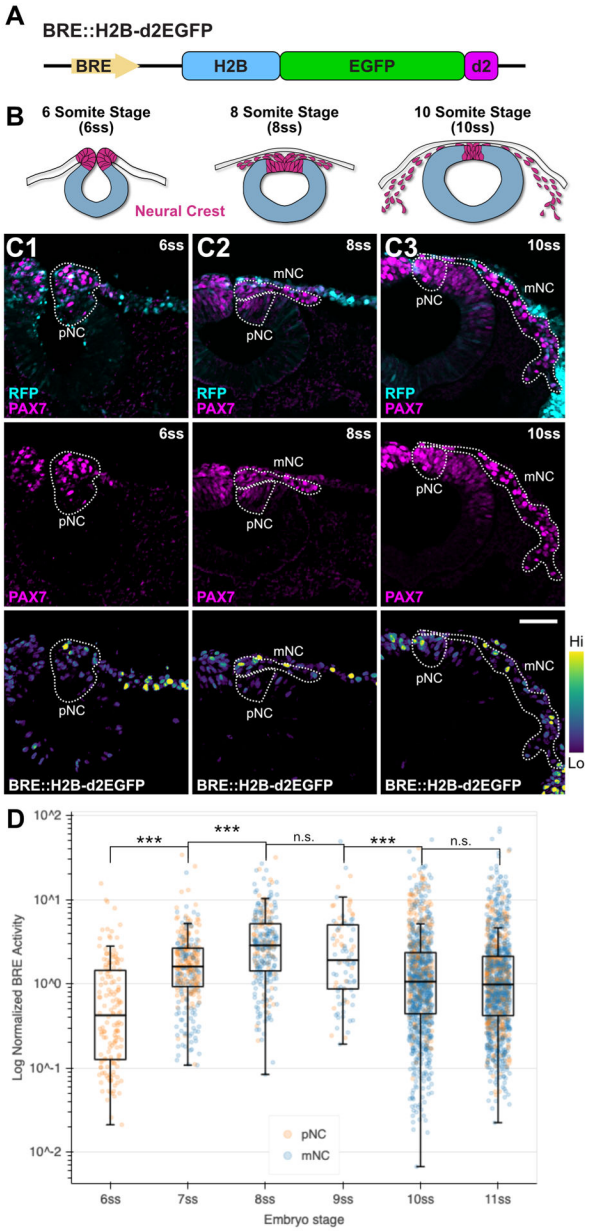

Figure 1: BMP signaling activity peaks during midbrain neural crest delamination.

(**A**) Schematic diagram representing the BMP-sensitive reporter construct used in this study. BMP-responsive elements (BRE) drive expression of histone H2B tagged with GFP harboring the destabilization domain from mouse ornithine decarboxylase (d2). (**B**) Schematic diagrams illustrating neural crest development in specified (6ss), delaminating (8ss), and migrating (10ss) neural crest cells at the midbrain axial level. (**C**) Gastrulating chicken embryos were electroporated with DNA constructs that ubiquitously express RFP (cyan) and BRE::H2B-d2EGFP (pseudocolored based on color scale on right), and examined at 6ss (C1), 8ss (C2), and 10ss (C3). Transverse sections were immunolabeled to label PAX7 expression in neural crest cells (magenta). Scale bar represents 50 μm. (**D**) BRE activity was measured within each PAX7-positive neural crest nucleus and normalized to RFP as an

electroporation control. *** $p<0.001$, n.s. not significant, Kruskal-Wallis one-way analysis with Bonferroni-adjusted Dunn's post-hoc analysis. ss, somite stage; pNC, premigratory neural crest; mNC, migratory neural crest.

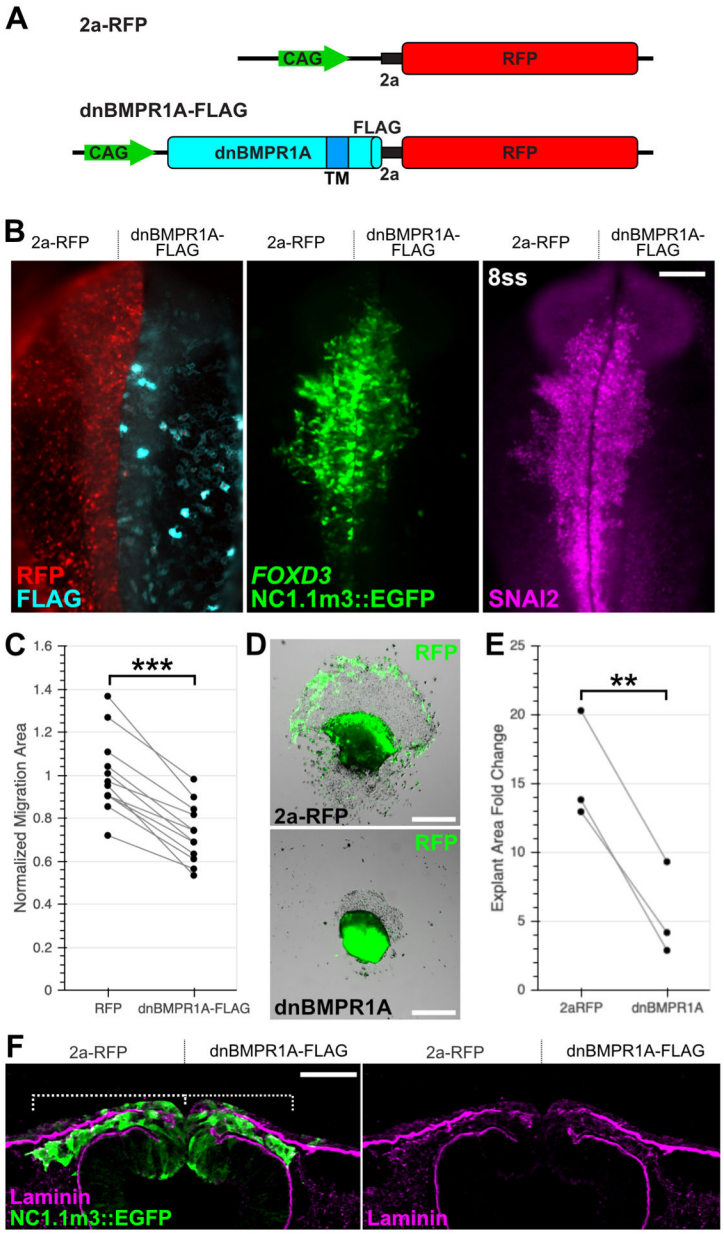

Figure 2: BMP signaling inhibition diminishes cranial neural crest migration

. (**A**) Schematic diagram of expression constructs used in this study. dnBMPR1A-FLAG (below) carries CAG-mediated expression of a dominant-negative, C-terminal truncated BMPR1A protein tagged with the FLAG epitope, followed by RFP translation downstream of a self-cleaving 2a peptide. 2a-RFP (above) serves as an electroporation control and is identical to the dnBMPR1A-FLAG construct without the dnBMPR1A-FLAG coding sequence. TM, transmembrane domain. (**B**) Gastrulating chicken embryos were electroporated with control 2a-RFP on the left side and dnBMPR1A-FLAG on the right side together with the *FOXD3* NC1.1m3 enhancer driving EGFP expression. Embryos were immunolabeled to display RFP (red), FLAG (cyan), EGFP (green), and SNAI2 (magenta) expression, and shown in whole mount. (**C**) Parallel coordinate plot displaying the

normalized neural crest migration area measured in whole mount, demonstrating a significant reduction in neural crest migration following BMP inhibition. *** $p<0.001$, two-tailed paired *t*-test, n=10 embryos. (**D**) Embryos bilaterally electroporated with 2a-RFP and dnBMPR1A-FLAG were incubated until specification stages (5ss) at which point dorsal neural tube explants were collected from the forming midbrain and cultured in imaging chambers. Displayed are overlays of brightfield and RFP images of one representative explant pair at 24 hours post explant (hpe). (**E**) Parallel coordinate plot displaying the explant area fold change as calculated by dividing 24 hpe area by 2 hpe area for control and BMP-inhibited explants, with lines connect values from explants collected from the same embryo. ** $p<0.01$, two-tailed paired *t*-test, n=3 explant pairs. (**F**) Representative transverse section of 8ss embryo immunolabeled for the laminin (magenta) demonstrates normal basement membrane remodeling following dnBMPR1A-FLAG expression (n=8/8 embryos). Dashed brackets in F illustrate neural crest migration distances. Scale bars represent 100 μm (A), 200 μm (D), and 50 μm (F). ss, somite stage.

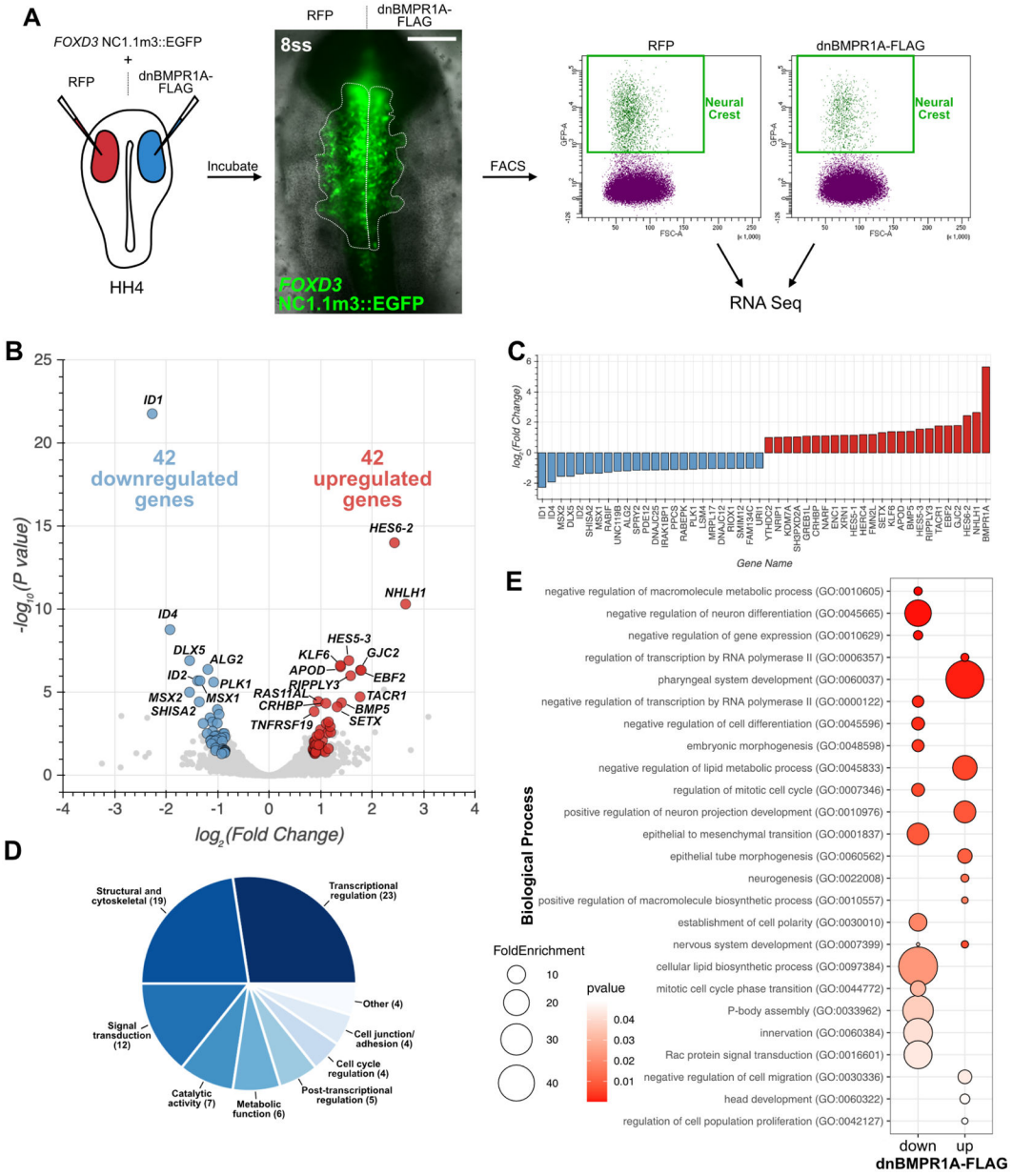

Figure 3: Transcriptome profiling reveals targets of BMP signaling during cranial neural crest EMT.

(**A**) Diagram of RNA-seq experiment pipeline. Embryos were electroporated with control 2a-RFP or BMP-inhibiting dnBMPR1A-FLAG together with the *FOXD3* NC1.1m3 enhancer driving EGFP expression. Embryos were then incubated to delamination stages (8ss) at which point embryos heads were dissociated and EGFP+ neural crest cells were isolated by fluorescence activated cell sorting and used for cDNA library preparation and sequencing. Scale bar represents 100 μm. HH, Hamburger-Hamilton stage; ss, somite stage. (**B**) Volcano plot displaying the differential gene expression analysis results. Downregulated genes (blue) reflect positive targets of BMP activity, while upregulated genes (red) reflect negative targets of BMP activity. See also Supplemental Figure 2 for additional gene labels. (**C**) Bar plot displaying differentially expressed genes with the highest fold change. (**D**) Pie

chart showing molecular function categories for differentially expressed genes. In parentheses are the number of dysregulated genes with each molecular function. (**E**) Bubble plot displaying a subset of enriched Gene Ontology (GO) Biological Processes in the down- and up-regulated gene sets. Bubble color reflects *p* value and size reflects fold enrichment compared with a random gene set.

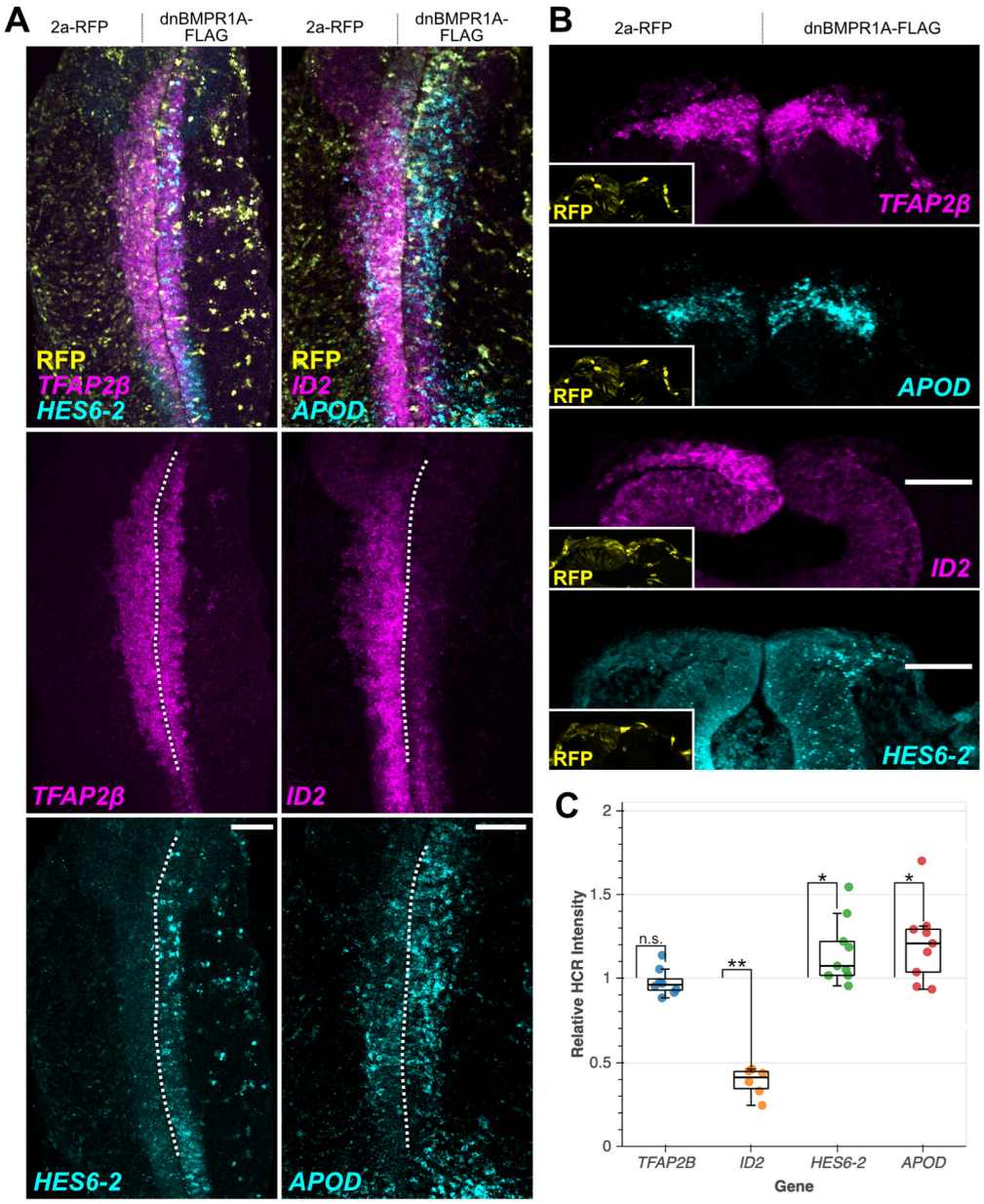

Figure 4: BMP signaling is required for expression of *ID2* and suppresses expression of *HES6-2* and *APOD*.

(**A**, **B**) Gastrulating chick embryos were electroporated with control 2a-RFP on the left and dnBMPR1A-FLAG on the right sides and were allowed to develop to neural crest delamination stages (8ss). Embryos were then fixed and processed for Hybridization Chain Reaction (HCR) to fluorescently label the indicated mRNA transcripts. Dashed lines indicate the embryonic midline. (**B**) Representative transverse sections of embryos in (A). Scale bars represent 100 μm (A) and 50 μm (B). (**C**) Boxplot shows the relative expression levels for each indicated gene as determined by dividing the fluorescence intensity on the BMP-inhibited side by the control side. ** $p<0.01$, * $p<0.05$, n.s. not significant, two-tailed paired

t-tests, *TFAP2B* n=8 embryos, *ID2* n=6 embryos, *HES6-2* n=9 embryos, *APOD* n=9 embryos.

KEY RESOURCES TABLE

Reagent or resource	Source	Identifier
Antibodies		
Mouse monoclonal IgG1 anti-Pax7	Developmental Studies Hybridoma Bank (DSHB)	Cat# PAX7, RRID:AB_528428
Mouse monoclonal IgG1 anti-Cadherin-6B	Developmental Studies Hybridoma Bank (DSHB)	Cad# CCD6B-1, RRID:AB_531766
Rabbit monoclonal anti-Slug (Snai2, Clone C19G7)	Cell Signaling Technologies	Cat# 9585, RRID:AB_2239535
Rabbit polyclonal anti-Sox9	Sigma-Aldrich	Cat# AB5535, RRID:AB_2239761
Rabbit monoclonal anti-Laminin (LAMA1)	Sigma-Aldrich	Cat# L9393, RRID:AB_477163
Mouse monoclonal IgG1 anti-FLAG (Clone M2)	Sigma-Aldrich	Cat# F1804, RRID:AB_262044
Rabbit anti-Phospho-Smad 1 (Ser463/465)/ Smad5 (Ser463/465)/ Smad9 (Ser465/467) (Clone D5B10)	Cell Signaling Technologies	Cat# 13820, RRID:AB_2493181
Goat polyclonal anti-GFP	Rockland	Cat# 600-101-215M, RRID:AB_2612804
Rabbit polyclonal anti-RFP/DsRed	MBL International	Cat# PM005, RRID:AB_591279
Deposited Data		
RNA-seq data: Cranial neural crest from Gallus gallus HH9+ dnBMPR1A-FLAG-expressing (replicate 1 and 2)	This paper	https://www.ncbi.nlm.nih.gov/sra/PRJNA717985
RNA-seq data: Cranial neural crest from Gallus gallus HH9+ control (replicate 1 and 2)	(Hutchins et al., 2021)	https://www.ncbi.nlm.nih.gov/bioproject/PRJNA673315
Experimental Models: Organisms/Strains		
Wild type fertilized *Gallus gallus* eggs	Sunstate Ranch, Sylmar, CA, USA	
Oligonucleotides		
Primer: H2B AscI FWD: ATATGGGCGGCCAAGCTTCGAATTGCGCACCA	This paper	
Primer: d2EGFP AscI REV: ATATGGCGCGCCAGAATCTAGAGGCTCGAGAG	This paper	
Primer: BRE AscI FWD: ATATGGCGCGCCCCCTAGAACTATAGTGAGTC	This paper	
Primer: BRE AscI REV: ATATGGCGCGCCCAAGCTCCTTGAATTCGAAT	This paper	
Primer: 2a-RFP FWD 1: CGGGGACGTGGAGGAAAATCCCGGCCCTGAAATGGCCTCCTCCGAGGACG	This paper	
Primer: 2a-RFP FWD 2: CTCCGGCGAGGGCAGGGGAAGTCTTCTAACATGCGGGGACGTGGAGGAAAATCC	This paper	

Reagent or resource	Source	Identifier
Primer: 2a-RFP FWD 3 ClaI: AGCTCATCGATGCCGCCACCATGGGCTCCGGCGAGGGCAGGGG	This paper	
Primer: RFP stop REV NotI: ATATGCGGCCGCTTAGGCGCCGGTGGAGTGGCG	This paper	
Primer: BMPR1A ATG XhoI FWD: ATATCTCGAGGCCACCATGACTCGACTGAGAGTTTGTGAGC	This paper	
Primer: dnBMPR1A-FLAG ClaI REV: GCGGCATCGATCTTGTCGTCATCGTCTTTGTAGTCGCCGGAGCCTGCTTCATCTTGTTCCAGGTCACG	This paper	
Recombinant DNA		
Plasmid: BRE::EGFP	(le Dréau et al., 2012)	
Plasmid: TCF/Lef::H2B-d2EGFP	(Piacentino et al., 2020)	
Plasmid: BRE::H2B-d2EGFP	This paper	
Plasmid: pCI H2B-RFP	(Betancur et al., 2010)	
Plasmid: pCAG::2a-RFP	This paper	
Plasmid: pCAG::dnBMPR1A-FLAG	This paper	
Plasmid: pTK-*FoxD3*-NC1.1m3::GFP	(Simões-Costa et al., 2012)	
Software and Algorithms		
Fiji v1.53c	(Schindelin et al., 2012)	https://imagej.net/Fiji
Bowtie2 v2.3.5.1	(Langmead and Salzberg, 2012)	http://bowtie-bio.sourceforge.net/bowtie2/index.shtml
Cutadapt v2.10	(Martin, 2011)	https://cutadapt.readthedocs.io/en/stable/
FeatureCounts v2.0.1	(Liao et al., 2014)	http://subread.sourceforge.net/
R v3.6.1	(Ihaka and Gentleman, 1996)	https://www.r-project.org/
RStudio v1.2.1335	(Racine, 2012)	https://www.rstudio.com/
DESeq2	(Love et al., 2014)	https://bioconductor.org/packages/release/bioc/html/DESeq2.html
Python v3.7.6	(van Rossum and Drake, 2009)	https://www.python.org/downloads/release/python-376/
Pandas v0.24.2	(McKinney and Team, 2015)	https://pandas.pydata.org/
Bokeh v1.4.0	(Bokeh Development Team, 2018)	https://docs.bokeh.org/en/latest/index.html
Iqplot v0.1.6	(Bois, 2020)	https://iqplot.github.io/index.html

Reagent or resource	Source	Identifier
Scipy v1.5.2	(Virtanen et al., 2020)	https://scipy.org/
Scikit_posthoc v0.6.5	(Terpilowski, 2019)	https://scikitposthocs.readthedocs.io/en/latest/
Numpy v1.19.2	(van der Walt et al., 2011)	https://numpy.org/devdocs/index.html
Seaborn v0.11.0	(Waskom, 2012)	https://seaborn.pydata.org/
Holoviews v1.13.3	(Stevens et al., 2015)	https://holoviews.org/